

Transient Analysis of Ionic Cluster Emission from a Silicon Surface by Nitrogen-Laser Excitation

A. Kasuya and Y. Nishina

The Research Institute for Iron, Steel and Other Metals, Tohoku University, Sendai 980, Japan

(Received 13 May 1985)

Ionic cluster emission from Si by nitrogen-laser excitation is observed in a range of peak intensity from 50 to 500 MW/cm². Spectral analysis of time-of-flight measurements suggests the presence of ionic clusters within nanoseconds of irradiation. These clusters initially have a nearly uniform mass-to-charge ratio between $\frac{3}{2}$ and $\frac{5}{4}$ in units of Si⁺, and decompose through numerous channels of fragmentation. The result is in remarkable contrast with those of measurements in a time scale of more than 10 μs with the mass distribution corresponding to quasithermal equilibrium.

PACS numbers: 79.20.Ds, 52.40.Hf, 64.60.Ht

Intense laser excitation on a solid surface induces ion emission.¹⁻⁵ In spite of extensive studies over the past twenty years, it has not been possible to quantify experimentally the chemical form of desorbed ions and their energy states of excitation immediately after emission from the surface. This Letter presents a new approach to this problem by transient mass analysis based on the line profile study on the time-of-flight (TOF) spectrum. The result with nitrogen-laser excitation shows that the ions are emitted from a Si surface initially in cluster forms which decompose mostly into individual ions in a time scale of 10 μs through numerous channels of fragmentation. Our analysis on the fragmentation process over a 100-ns period gives the result that the mass-to-charge ratio, M/q , immediately after emission lies in the range $\frac{5}{4} \leq M/q \leq \frac{3}{2}$, where M is the number of Si atoms and q is the ionic charge in units of electron charge.

Repetitive emission of ions from the (111) surface of Si is analyzed by a TOF spectrometer under pulsed nitrogen-laser irradiation in the peak intensity range from 50 to 500 MW/cm² (photon energy, 3.68 eV; pulse width, 10 ns). The spectrometer consists of a set of accelerating electrodes followed by a straight drift tube 62 cm long.⁴ The straight ion trajectory allows us to analyze the decomposition of emitted ions. The potential of 300 V is applied between the sample and the entrance aperture (distance, 2.5 cm) of the drift tube. The sample surface is cleaned directly by electrical Joule heating in the vacuum of less than 10⁻⁷ Pa. It is a characteristic feature of the ion emission in the above range of excitation that the line profile of the TOF spectrum fluctuates appreciably for a given intensity level of laser beam incident repetitively on the same area of the sample surface. Figure 1 shows several spectra of representative forms as recorded separately for each laser shot with its peak intensity of 200 MW/cm² over the sample area of 4 × 10⁻⁵ cm². Below this intensity the efficiency of ion emission decreases drastically. That is, no ion emission is observed for appreciable numbers of laser shots out of

the total. In spite of the wide varieties of spectral shapes, the following features are common to all the spectra: (1) In this intensity range the total number of emitted atomic ions is found in excess of 10³. (2) The TOF spectrum exhibits a continuous yield of ions in the flight-time region between Si⁺ (13.7 μs) and Si₂⁺ (19.3 μs). This continuous spectrum is in remarkable contrast with our previous result on graphite in which a series of sharp lines are observed.⁴ (3) The leading edge, t_1 , and the trailing edge, t_2 , of a spectrum are considerably sharp in comparison to its width, $w = t_2 - t_1$. (4) There is a definite correlation in the spectra that the shorter t_1 is, the longer the t_2 of the same spectrum. (5) The wider w is, the higher the integral intensity of the spectrum. Figure 1 displays these features, particularly (4) and (5), in the increasing order of spectral area from (a) through (f) with their t_1 's (t_2 's) becoming shorter (longer). (6) Both edges of the spectrum are connected with a smooth tail on which weak peaks and shoulders are superposed. (7) An independent measurement by a quadrupole mass spectrometer (QM) in the time scale of 10 to 100 μs under a similar excitation condition shows that Si⁺ is the only dominant species and Si₂⁺ and others are at least 1 order of magnitude smaller than Si⁺ in the

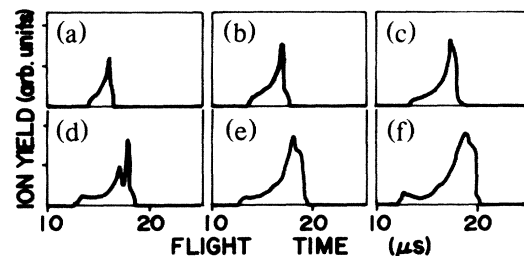


FIG. 1. Time-of-flight spectra of ions emitted from the (111) surface of Si by nitrogen laser excitation at the peak intensity of 200 MW/cm² averaged over the cross section of the beam. These spectra are selected out of hundreds of measurements and are displayed in order of increasing spectral width and intensity from (a) through (f).

spectral intensity.²

Figure 2 shows those common characteristics deduced from TOF spectra as described in the spectral features (2) through (5) by plotting t_1 and t_2 vs w . Each spectrum gives the values of t_1 , t_2 , and w . The t_1 and t_2 are plotted as a pair of data points on a common vertical line which crosses the value of w on the abscissa. The spectral feature (4) is clearly shown in this figure. One should note that the distribution of data points shown in Fig. 2 is statistically reproducible in the following sense: The maximum fluctuation of t_1 (t_2) for $w = 6 \mu\text{s}$ is found to be less than $\pm 5\%$. This fluctuation, however, decreases with decreasing w down to less than 3% for $w = 3 \mu\text{s}$.

The spectral width shown in Fig. 1 is not due to a degradation of TOF spectrum caused by the spread in the initial kinetic energy of ions nor by the space charge built up in the acceleration field. The maximum initial energy of ions is found to be typically less than 30 eV as estimated from three separate measurements; i.e., (i) the TOF spectrum at $V_d = 0$, (ii) time-resolving analysis of ions passing through a 127° electrostatic energy analyzer (EA), and (iii) that by QM spectrometer. Hence the initial energy spread amounts to a spectral uncertainty less than 5% of t_1 . The space-charge effect is also negligible because the ion current density of our measurement amounts to less than 1% of the saturation limit caused by the space charge. Since the wide spectral width is not caused by extrinsic effects as shown above, it has to come from decomposition of emitted ions within the period of acceleration in the spectrometer.⁶ This period is 890 ns for Si^+ with its initial energy of 30 eV under the experimental condition of Fig. 1. Among those spectra shown in Fig. 1, (a) and (b) are the simplest in spectral profile and exhibit fundamental components of spectral forms (c) through (f). Each of the spectra (c) through (f) consists of two or more of the profiles (a) with their respective values of t_1 , t_2 , w , and total area.

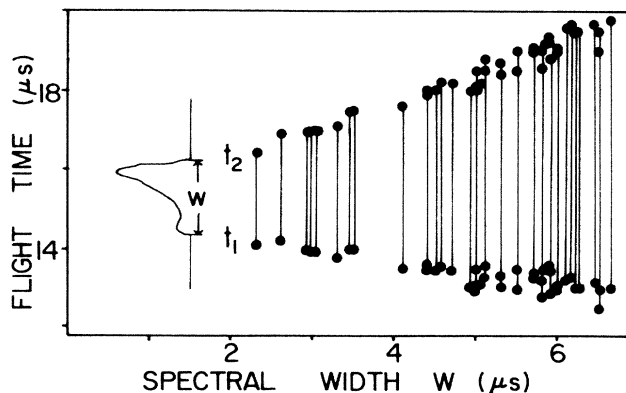


FIG. 2. Plot of the leading edge t_1 and the trailing t_2 of each spectrum vs the spectral width $w = t_2 - t_1$. The vertical line connects t_1 with t_2 of the same spectrum.

The profile (a) can be explained in terms of a decomposition process, $\text{Si}_k^{a+} \rightarrow \text{Si}_m^{b+} + \text{Si}_n^{c+}$, where the inequality $n/c \geq k/a \geq m/b$ holds with an auxiliary condition $n/c \geq m/b$, because of the conservation of charge, $a = b + c$, and of the mass, $k = m + n$. Suppose that this process occurs with $N \text{Si}_k^{a+}$ ions at the rate given by $dN/dt = -N/\tau$ (τ is the decomposition time which is comparable to the acceleration period). Those ions which decompose into Si_m^{b+} and Si_n^{c+} immediately after their emission contribute to the spectral leading edge at the flight time for Si_m^{b+} and to the trailing edge at the flight time for Si_n^{c+} . Because of the inequality on mass-to-charge ratio, these edges always appear on both sides of the spectral position of the flight time for the parent ion, Si_k^{a+} , which would exhibit a peak if it did not decompose in the acceleration field before reaching the entrance aperture of the drift tube. The parent ions which decompose while flying in the drift tube should give rise to this peak, because the kinetic energy released to those fragments is negligible compared to the total kinetic energy gained by the parent from the acceleration field. Those ions which decompose while in the acceleration field give rise to a continuous distribution of tails from these edges toward Si_k^{a+} . The spectrum, therefore, exhibits a sharp leading edge for Si_m^{b+} as well as a trailing edge for Si_n^{c+} , both connected with smooth tails toward Si_k^{a+} . This spectral feature is consistent with the observed line profiles shown in Figs. 1(a) and 1(b). Even if the parent ion decomposes into more than two fragments simultaneously, the fragment with the smallest (largest) M/q gives rise to t_1 (t_2) while the other fragments contribute to the spectral features between them.

Under these circumstances, positions of spectral edges depend on the following three parametric conditions: (A) M/q of the parent ion, (B) M/q 's of fragments according to the way the parent breaks up, and (C) time evolution of decomposition. Figure 2 shows that the distribution of points for t_1 and that for t_2 can be extrapolated to a common point around $t_0 = 15 \mu\text{s}$ at $w = 0$. The smooth distribution of data points shows that the pair of points t_1 and t_2 observed for each spectrum take positions close together or far apart by an out-of-phase displacement with respect to t_0 . If the condition (A) were to vary for each event of laser desorption, t_1 and t_2 in the spectrum would shift more or less together in phase (not out of phase) in the same direction as the shift of t_0 for the parent ion. If M/q 's of fragments were different from event to event for a given M/q of the parent, t_1 and t_2 would change their values independently of each other according to the way the parent ion breaks up. None of these features appears in the results shown in Fig. 2. Thus the correlation between t_1 , t_2 , and w as shown in Fig. 2 is a direct consequence of the fact that the conditions

(A) and (B) of the decomposition process are quite similar in all of the parent clusters giving rise to these points. Then, only (C) varies from event to event of laser desorption.

The time evolution of decomposition process [condition (C)] can be conceived for the two extreme cases for emission of thousands of atoms or ions by one laser shot: In process I, atoms or ions are emitted as a large number of small molecules like ionized gas consisting of dimers or trimers of Si; in process II, they are initially divided up into a relatively small number of large clusters, like a droplet or a macromolecule. Since the number of emitted ions is large in process I, the TOF spectrum would exhibit a distribution corresponding to the statistical average of the decomposition processes, so that one should observe an identical spectrum for each desorption event for a given intensity level of incident laser beam, in contradiction with our results. In process II, on the other hand, the TOF spectrum does not represent the statistical average of the fragmentation, because it reflects the decomposition processes of only a small number of ionic clusters at a time. Since a large cluster can decompose through numerous fragmentation channels, a hundred examples of our measured spectra are still insufficient to exhaust all the possible profiles. According to this interpretation, the varieties of our TOF spectrum in Fig. 1 have a definite physical significance. The spectral width w depends on a composite time constant of decomposition in process II, representing a measure of how rapidly the fragmentation of clusters proceeds toward their ultimate form of monoatomic ions. The more rapidly the fragmentation proceeds, the more readily do M/q 's of fragments differ from that of the parent in the acceleration field of TOF spectrometer, and thereby the wider does the spectral width w become. As mentioned previously (see Fig. 2), the fluctuation in t_1 (t_2) for a given w increases with w , because the larger w is, the more the possible fragmentation channels. In the limiting case $w = 0$, a substantially long time is required for decomposition so that the corresponding $t_1 = t_2 = t_0$ represents M/q of the parent. From the value of t_0 at $w = 0$, one can deduce M/q of the parent cluster in the plot of Fig. 2 to be in the range $\frac{5}{4} \leq M/q \leq \frac{3}{2}$. The parent cluster with this value of M/q is formed in a period less than the first 100 ns after laser excitation, because our measurement can detect decomposition process in that time scale. Hence, the 10-ns laser irradiation is regarded as instantaneous in our analysis. In Fig. 1 the sharp spectral edges imply that the time evolution of the decomposition process is quite similar among clusters out of a single pulsive event of desorption, whereas the variety of spectra in separate events suggest that the evolutions are rather dissimilar from each other.

Further evidence for the decomposition of process II

can be found through the V_d dependence of the TOF spectrum. Since the increase in V_d is to reduce the flight time of ions passing through the acceleration field between the sample and the entrance aperture of the drift tube, the spectrum reflects only earlier stages of decomposition process in its distribution. In the above analysis on the results in Fig. 2, data points of hundreds or so are regarded as equally probable and are sufficiently large in number to represent their statistical distribution. Figure 2, however, shows that the distribution of data points is concentrated mostly on the value of w near $6 \mu\text{s}$. For the measurement with $V_d = 300 \text{ V}$, the number of data points (number of occurrences) for a given segment of w increases as w increases from zero, exhibits a maximum at $w_p = 5.8 \mu\text{s}$, and then decreases sharply to zero with further increase in w . A similar and reproducible distribution curve is obtained for each series of measurements for different values of V_d . Figure 3 shows the plot of t_1 and t_2 vs $V_d^{-1/2}$ for the spectrum having the width w_p for the highest number of occurrence for a given V_d . In a low range of V_d ($< 500 \text{ V}$), t_1 and t_2 are found approximately on the lines drawn for Si^+ and Si_2^+ , respectively. As V_d increases, these values tend to become closer to each other in a few discrete steps and exhibit similar (out-of-phase) deviations from the two lines. This result shows that ionic clusters decompose through several consecutive steps so that as V_d increases, each step in the change of the spectrum represents a transition to the fragmentation process of the previous stage. These observations are well predicted in the decomposition of process II but are inconsistent with process I. In process I, one expects to

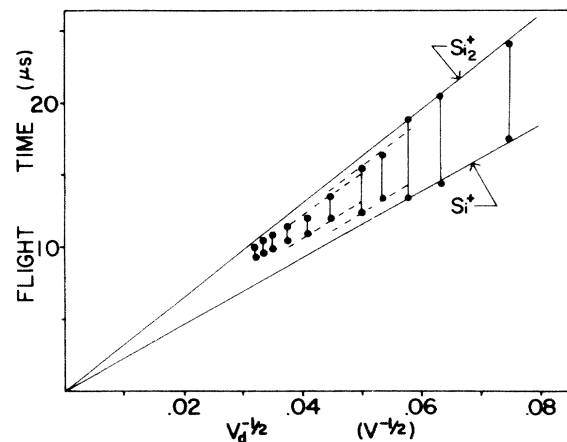


FIG. 3. Plot of t_1 and t_2 vs $V_d^{-1/2}$ applied between the sample and the entrance aperture of the drift tube for the distance of 2.5 cm. The straight lines indicate the flight time of Si^+ or Si_2^+ as a function of V_d . The steplike deviations of data points from these lines suggest the presence of composite decomposition process. The dotted lines are drawn to indicate this effect.

observe a peak for the parent between the spectral edges since there would be always a finite probability for some of the parent ions to pass through the acceleration field of the spectrometer without experiencing decomposition. This probability would increase with increasing V_d so that the parent peak would increase in intensity relative to the contribution from fragments. Our spectrum, on the other hand, does not show any sign of such a peak at all for $V_d = 300$ V (see Fig. 1) and even at the largest $V_d = 2000$ V. This must be the case for process II, because the parent cluster ceases to exist at the very first step of decomposition, leaving no trace in the spectrum.

For confirming our TOF analysis, we have performed an independent measurement for finding the flight-time distribution of emitted clusters which pass through EA. The result shows that the fragmentation continues to take place in a time scale over $10 \mu\text{s}$. Furthermore, the spectral distribution is consistent with that predicted by extrapolation toward longer flight time of our TOF measurements and, on account of conservation of total charge and mass, it explains the fact that the M/q or the original cluster lies between $\frac{5}{4}$ and $\frac{3}{2}$. This result also interrelates the results of our TOF measurements to those of QM, each of which deals with different time domains of fragmentation ranging from 0.1 to $10 \mu\text{s}$ or longer.

Though our TOF measurement does not yield direct information on the initial size of a cluster in process II, its approximate lower limit can be deduced from the distribution of data points in Fig. 2. One can estimate the number of possible fragmentation channels for a given cluster which decomposes through a series of successive disintegration of the type $\text{Si}_k^{a+} \rightarrow \text{Si}_m^{b+} + \text{Si}_n^{c+}$ ($a = b + c$, $k = m + n$) down to final products of singly charged ions. Assuming a characteristic decomposition time τ_i ($i = 1, 2, 3, \dots$) for each step in the series of above disintegration processes, one obtains the maximum number of observable spectral shapes which is equal to the calculated number of fragmentation channels, with their respective values of t_1 , t_2 , and w in the spectrum. In our conservative estimate on the Si clusters of

$M > 10$, there should be at least 22 channels of fragmentation, suggesting the numerous types of line shapes of our spectra, e.g., Figs. 1(c)–1(f), for $M \gg 10$.

In conclusion, we have found that ionic clusters with an initially common value of mass-to-charge ratio are emitted from solid surface of Si by pulsed nitrogen laser excitation. Similar phenomena are also observed in Ge, Sn, and Pb with nearly equal values of M/q as in Si.^{7,8} Our method of analysis can deduce their subsequent decomposition process in a submicrosecond scale from the line profile of our TOF spectrum measured in $10\text{-}\mu\text{s}$ scale. The laser desorption process in our range of excitation intensity and energy density is distinctively different from any other desorption phenomena described in terms of a single-particle excitation or of ordinary evaporation.

Authors would like to thank Professor K. Ohno of Hokkaido University, Professor C. Horie, and Professor M. Tachiki of Tohoku University for valuable discussions. This work was supported in part by the Grant-in-Aid for Scientific Research from the Ministry of Education in Japan.

¹J. F. Ready, *Effects of High Power Laser Radiation* (Academic, New York, 1971).

²N. Furstenau and H. Hillenkamp, *Int. J. Mass. Spectrom. Ion Phys.* **37**, 135 (1981).

³*Laser Annealing of Semiconductors*, edited by J. M. Poate and W. Mayer (Academic, New York, 1982).

⁴A. Kasuya and Y. Nishina, *Phys. Rev. B* **28**, 6571 (1983).

⁵L. A. Bloomfield, R. R. Freeman, and W. L. Brown, *Phys. Rev. Lett.* **54**, 2246 (1985).

⁶B. T. Chait and F. H. Field, *Int. J. Mass Spectrom. Ion Phys.* **41**, 18 (1981).

⁷A. Kasuya and Y. Nishina, in *Secondary Ion Mass Spectrometry. SIMS IV*, edited by A. Benninghoven *et al.*, Springer Series in Chemical Physics Vol. 36 (Springer, Berlin, 1984), p. 164.

⁸A. Kasuya and Y. Nishina, in *Beam-Solid Interactions and Phase Transformations*, edited by H. Kurz, G. L. Olson, and J. M. Poate (Materials Research Society, Pittsburgh, PA, 1986); also see the abstract A2.4 of the meeting.